

**GEOMORPHOLOGY OF SHORTENING STRUCTURES ON MERCURY DEPICTS NO GROUPING INTO CATEGORIES.** Stephan R. Loveless<sup>1</sup>, Leta R. McCullough<sup>2</sup>, Christian Klimczak<sup>1</sup>, Kelsey T. Crane<sup>2</sup>, Paul K. Byrne<sup>3</sup>, <sup>1</sup>Center for Planetary Tectonics, University of Georgia Athens, 210 Field St. Athens, GA 30602 – [Stephan.loveless@uga.edu](mailto:Stephan.loveless@uga.edu), <sup>2</sup>Department of Geosciences, Mississippi State University, 214 Hilbun Hall, Mississippi State, MS, 39762, <sup>3</sup>Department of Earth and Planetary Sciences, Washington University in St. Louis, St. Louis, MO 63130.

**Introduction:** All terrestrial objects host shortening landforms on their surfaces. Such structures are commonly identified from morphological parameters, such as surface-breaking thrusts, scarps, and positive topographic relief that form ridge-like shapes. However, the individual parameters of thrust fault-related landforms, such as size, length width, and cross-sectional symmetry, are known to vary widely. Without *in situ* observation, the underlying architecture of shortening landforms is often interpreted as a simple (set of) thrust fault(s), even though a century of field observations of such structures on Earth show them to be very complex (e.g. [1]).

Many previous studies have grouped shortening landforms on Mercury into three categories based on qualitative descriptions (e.g. [2–5]):

- “Lobate scarps” are linear or bow-like surface-break structures described as having a steeply sloping forelimb and a gradually sloping backlimb;
- “Wrinkle ridges” are low-relief, broad and sinuous ridges that vary in geometry along their strikes, frequently showing a superposed secondary ridge (i.e., the wrinkle); and
- “High-relief ridges” are similar to lobate scarps but are described as having a greater relief and a steeper backlimb along their length.

Shortening landforms on the surface of Mercury have commonly been fit into more than one of these categories or exhibit characteristics of one category but transition to characteristics of another along strike (e.g. [6]), suggesting that these features do not readily fit single, discrete categories [7].

Currently, there is no quantitative distinction that relates the morphologic parameters of a shortening landform to one of the three traditional qualitative categories used in the literature. Here, we collate morphological measurements of 100 shortening structures on Mercury to assess if the traditional categories exist and quantify the parameters that govern the variability observed across shortening structures.

**Methodology:** To quantitatively assess the geomorphology of shortening landforms on Mercury, we first collected digital elevation models (DEMs) and global mosaics of Mercury from the MESSENGER mission available in the Planetary Data System (PDS) and DLR [8] and loaded them into a geographic

information system (GIS) using ArcMap 10.8. We then divided the Mercury data into a  $20^\circ \times 20^\circ$  grid, with 100 grid boxes selected at random. We selected one structure from each grid box based on data quality, coverage, and representation of the three traditional categories; once selected, we reproject the map view to the center of the landform using a stereographic projection.

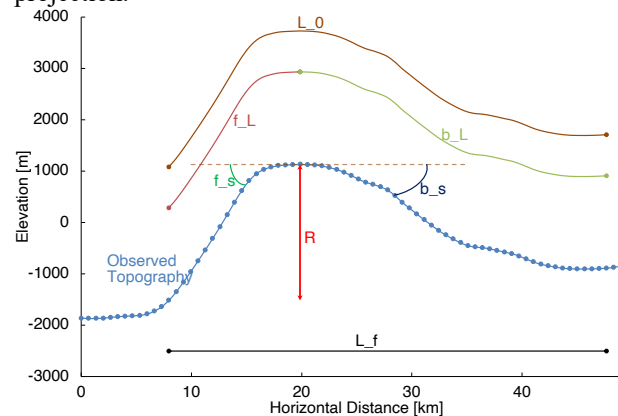


Fig. 1: Parameters recorded along an example transect across Calypso Rupes, showing a positive relief landform.

Each landform was mapped by tracing the scarp using a streaming mode with a vertex spacing of 500 m at a viewing scale of 1:250,000. The geodesic lengths ( $L$ ) of the map traces were extracted from the GIS for further analysis. Topographic cross sections were extracted from transects that are drawn perpendicular to landform strike at  $\sim 10$  km intervals. Assessments of the map and the cross sections allowed us to determine the maximum relief ( $R_{\max}$ ). In addition to  $L$  and  $R_{\max}$  values, the following parameters were extracted from all  $R_{\max}$  cross sections (see Fig. 1):

- Breadth, or horizontal distance across the transect, interpreted as the final, or deformed length of the transect ( $L_f$ , Fig. 1);
- Total (true) cross-sectional length of the transect, interpreted as the initial, undeformed length of the transect ( $L_0$ , Fig. 1);
- Average slopes of the forelimb and backlimb ( $f_s$  and  $b_s$  respectively, Fig. 1), calculated by finding the linear slope of each segment of the transect (shown as the line segments between points along the Observed Topography curve in Fig. 1) and taking their average along the entire forelimb or backlimb;

- Cross-sectional lengths of the fore- and backlimbs ( $f_L$  and  $b_L$  respectively, Fig. 1), which, if summed together, equals the total cross-sectional length of the transect;
- Symmetry of the transect, found as the difference between the forelimb and backlimb slopes ( $sym$ ); and
- Shortening strain of the landform, derived from the breadth and total cross-sectional length of the transect ( $Str$ );  $= 1 - L_f/L_0$ .

A principal component analysis (PCA) was then performed on these observational parameters to assess clustering caused by geomorphological observations. A PCA is a multivariate statistical tool that reduces the dimensionality of data with large sets of variables into principal components (PCs) to assess: 1) which variables have the most influence on the data's variance; and 2) any plausible clustering that may be found amongst the data from variance found between the data's parameters. The influence of each parameter on the principal components is then used to determine which parameters dictate the variability observed across the data set.

**Results:** The PCA shows that most of the variation in the data can be explained with two principal components (PC's, or axes). The effect of each of the parameters on these PC's (loadings) is demonstrated by the red arrows in Fig 2. The length of the arrow describes the strength of a parameter's correlation to a PC, and the direction depicts whether the correlation is negative or positive. For instance, the relief,  $R$ , has a strong negative correlation with PC 1, and a weaker, positive correlation with PC 2. The PCA shows that the final length ( $L_f$ ), initial length ( $L_0$ ), and relief ( $R$ ) of these shortening landforms have the most influence on observed geomorphic variability. Shortening strain, and the fore- and backlimb slopes also show strong influence on observed variability.

The biplot (Fig. 2) of the PCA is constructed from the first two principal components (PC 1 and PC 2), which explain the majority of variability in our data. The biplot shows one broad cluster of data points and does not produce any distinct clustering into two or more groups (Fig. 2) that would indicate if any categories of shortening landform types can be discretely classified. This finding, in turn, indicates that there is no distinction between wrinkle ridges, high relief ridges, and lobate scarps as defined by the morphologic parameters used in this study. Importantly, the distinction of groups in a PCA is limited to visual assessment of how the data is organized based on the intercorrelated variability of the data across its parameters.

**Future work:** Other statistical tools, like a discriminant function analysis, will be tested and may

yield more insight into what set of parameters govern the landform type. Furthermore, additional parameters, such as the curvature of the map trace or vergences of fault-related folds and their changes along the landform, would further aid in landform assessment.

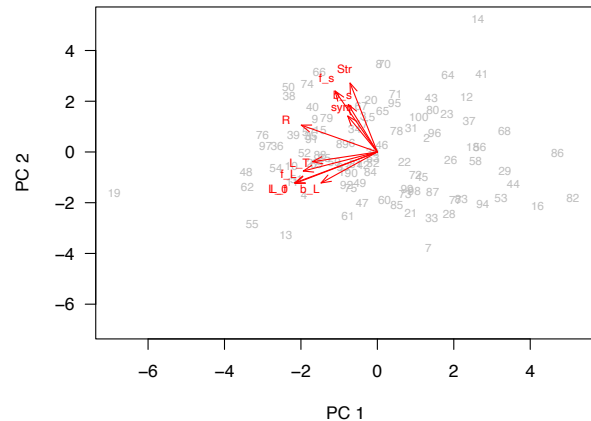


Fig. 2: Biplot of PCA. Gray numbers depict a contractional landform. Number is the landform's unique ID. Red arrows depict loadings of the parameters.

In the future, we also plan to select 50 shortening structures out of the ones presented here and model their underlying fault geometries. The Move-on-Fault algorithm of the MOVE software from Petroleum Experts will be used to model the underlying fault geometry of these 50 landforms, from which fault parameters will be extracted. In a preliminary study, we determined the underlying fault geometry for an exemplar shortening landform, finding that the fault has a listric geometry with an average dip angle of  $9.3^\circ$ . The results of the modeling phase of this work will be used for an additional multivariate statistical analysis to further assess shortening structure variability on Mercury.

**Acknowledgments:** This research is funded by NASA's SSW program. We make use of 14 PDS data products from the MESSENGER mission (<https://pds-imaging.jpl.nasa.gov/search/>). We thank Petroleum Experts for donating a MOVE suite software academic license to the University of Georgia.

**References:** [1] Boyer, S. and Elliot, D., (1982) *AAPG Bulletin*, 66, 1196–1230. [2] Dzurisin D. (1978) *JGR*, 83, 4883–4906. [3] Melosh, H. J. and McKinnon, W. B. (1988) *Univ. of Arizona Press*, 374–400. [4] Strom R. G. et al. (1975) *JGR*, 80, 1896–1977. [5] Watters et al. (2004) *GRL* 31, L04701, 1–5. [6] Klimczak C. et al. (2019) *Can J. Earth Sci.* 56, 1437–1457. [7] Byrne P. K. et al. (2018) In *Mercury: The View after MESSENGER* (Eds. Solomon S. C. et al.), 249–286. [8] Preusker F. et al. (2011) *PSS*, 59, 1910–1917.